

# Stabilization of Chaos in a Cancer Model: The Effect of Oncotripsy

Serpil Yilmaz

**Abstract**—There has been much interest in the development of therapies for the prevention and treatment of tumours. Recently, the method of oncotripsy has been proposed to destroy cancer cells by applying the ultrasound harmonic excitations at the resonant frequency of cancer cells. In this study, periodic disturbances whose frequency tuned to the fundamental frequency and the higher harmonics of the change in the population of tumor cells are applied to a tumour growth model, respectively, and the appearance of periodic behaviors in a three-dimensional chaotic cancer model is investigated as a result of those harmonic excitations. The numerical results show that by choosing the appropriate values of the parameters of periodic disturbances, the chaotic cancer model induces periodic behaviors such as period-one and two limit cycles which may have important implications on cancer treatment. The results also provide a view to understanding the oncotripsy effect within the framework of stabilization of chaos.

**Index Terms**—Bifurcation, cancer model, chaos, stabilization.

## I. INTRODUCTION

CANCER is a disease that is caused by abnormal or uncontrolled cell growth. Understanding the mechanisms of tumour growth is an actively developing field among many researchers from different disciplines. There are several techniques that are used to perform cancer diagnosis such as X-ray mammography, magnetic resonance imaging, ultrasound technique, digital tomosynthesis, and microwave imaging [1–4]. There are also many mathematical models about tumour-immune dynamics which have been extensively studied to provide valuable insights into the evolution of tumours. A deterministic model in the form of second-order ordinary differential equations governing the populations of immune cells and the tumour cells has been proposed in [5]. There have been many other studies on deterministic tumour-immune models [6–11]. A bifurcation analysis has been developed in [12] to explore the effect of immune response and the treatment strategy of periodically pulsed therapies on tumour-immune dynamics. Pulsed immunotherapy has been extended and a novel hybrid model combining chemotherapy and immunotherapy has been proposed in [13] and the effects of duration, dosage and frequency of combined treatment strategies have been investigated on the tumour population. The above studies have been obtained based on the deterministic tumour-immune model. However, in recent years, stochastic models of tumour-immune systems have been also developed.

Serpil YILMAZ is with Department of Computer Engineering and Artificial Intelligence & Data Science Research and Application Center, İzmir Katip Çelebi University, İzmir, 35620 Türkiye, (e-mail: [serpil.yilmaz@ikcu.edu.tr](mailto:serpil.yilmaz@ikcu.edu.tr))

 <https://orcid.org/0000-0002-6276-6058>

A tumour-immune model driven by symmetric Lévy noise has been studied in [14]. The effects of noise intensity and stability index have been analyzed on the tumour growth dynamics and the numerical results showed that the effects of Lévy stable noise lead to a decrease of the tumour cells compared with the Gaussian noise. A stochastic mathematical model of the coevolution of immune- and tumour cells has been proposed in [15] by considering both interactions and phenotypic plasticity to help guide the treatment protocols. By considering the variability in cellular reproduction, death and the fluctuation of chemotherapy effect, the deterministic differential equation model has been extended to the stochastic one to analyze the dynamics of tumour cells and immune cells under chemotherapy in [16]. The culling rate of effector cells and the intrinsic growth rate of tumour cells have been modeled as stochastic processes and the effect of environmental noise on the dynamic behaviors of the tumour-immune model has been studied in [17]. A stochastic tumour-immune system with a combination of immunotherapy and chemotherapy has been modeled in [18] and the evolution of tumours has been analyzed in the presence of environmental noise and chemotherapeutic dose. The responses of tumour growth to different drug dosing frequencies have been studied in [19] to improve treatment success.

Despite the various treatment modalities in practice such as radiotherapy, chemotherapy, immunotherapy, or their combination, there is a constant search for alternative modes of treatment for cancer. In [20] a new cancer therapy which is referred to as oncotripsy has been proposed by applying the low-intensity ultrasound waves at specific resonance frequencies. The method is based on the differences in morphologies and material properties between the healthy and tumour cells to selectively target cancer cells. Since the resonant frequency is generally obtained by geometric configurations and the mechanical properties of individual cells such as shape, size and stiffness which are altered in disease then the natural resonant frequencies of healthy cells should be significantly different from those of cancer cells. Therefore, the natural frequency of cells can be used as a tool for specifically targeting the cancer cells while sparing the healthy cells. The normal and cancer cells have been modeled as a sphere linear elastic material in [21] and modal analysis has been carried out to determine the natural frequencies of the cells. Frequency responses of healthy and cancer cells to mechanical stimuli (typically low-intensity therapeutic ultrasound) have been studied in [22] and it has been shown that the discrimination of the normal and tumour cells can be amplified at some ultrasound frequencies. The influence of viscoelasticity on the oncotripsy effect has been studied in [23]. A new perspective for cancer

treatment has been studied in [24] based on utilizing resonance interaction mechanisms between an applied electromagnetic field and the resonant frequency of cancer cells. The effect of thermodynamic resonance in the presence of electromagnetic waves with resonant frequency has been experimentally tested in [25] and it has been shown that cancer cell invasion and proliferation can be decreased with the specific electromagnetic field. The method of oncotripsy has been studied in a panel of breast, colon, and leukemia cancer cell models in [26, 27] by conducting mechanistic experiments. A three-dimensional dynamics of the cell has been developed in [28, 29] and the numerical experiments of the dynamic response of a cell in the presence of ultrasound waves have been presented.

Furthermore, the interactions between tumour and immune cells are nonlinear and extremely complicated which exhibit many properties of chaotic systems. A simple tumour growth model which has chaotic behavior in the parameter range of interest has been developed in [11]. The relationship between tumour size and the chaotic behavior of system dynamics has been examined in [30]. The chaotic behavior has been analyzed in a stochastic cancer model in [31] in which Brownian motion has been used to obtain the corresponding stochastic model with the spread of cancer. As it is well known, even a small disturbance in chaotic systems may lead to a significant change in the nature of the system behavior.

With the above discussions, the aim of this study is to analyze the stabilization of chaotic behavior in the presence of some external periodic disturbances. Our research question is therefore how the dynamics of tumour cells evolve if periodic disturbances are applied at the natural resonant frequency of the change in the population of tumour cells. The effects of fundamental frequency and higher harmonics on the periodic behavior of the cancer model have been also compared. To the best of our knowledge, this is the first study to investigate the effect of oncotripsy in a chaotic cancer model.

The paper is organized as follows. In Section II, the dynamics of a chaotic cancer cell have been modeled in the presence of periodic disturbances. In Section III, the fundamental frequency and higher harmonics of the change in the population of tumour cells have been calculated. The bifurcation analysis has been carried out and the dynamic responses of the model have been obtained numerically. The discussions of the analysis have been presented in Section IV.

## II. THE CANCER MODEL IN THE PRESENCE OF PERIODIC DISTURBANCES AT HARMONICS

Periodic disturbances have been applied to the cancer model proposed in [11] which is described by the system of differential equations given as:

$$\begin{aligned} \frac{dT}{dt} &= r_1 T \left(1 - \frac{T}{k_1}\right) - \alpha_{12} TH - \alpha_{13} TE + g(t) + \epsilon \xi(t) \\ \frac{dH}{dt} &= r_2 H \left(1 - \frac{H}{k_2}\right) - \alpha_{21} TH \\ \frac{dE}{dt} &= \frac{r_3 TE}{T + k_3} - \alpha_{31} TE - d_3 E \end{aligned} \quad (1)$$

where  $T(t)$  is the number of tumour cells at time  $t$  with the growth rate of  $r_1$  and maximum carrying capacity  $k_1$ .  $H(t)$  is the number of healthy cells at time  $t$  with the growth rate of  $r_2$  and maximum carrying capacity  $k_2$  and  $E(t)$  is the number of effector immune cells at time  $t$ . The parameters  $\alpha_{12}$  and  $\alpha_{13}$  denote the tumour cells killing rate by the healthy cells and effector cells, respectively. The parameter  $r_3$  denotes the effector cell production rate in response to the presence of tumour cells. The parameter  $d_3$  is the decay rate of effector cells and  $k_3$  is the half-saturation constant rate for immune production. The rates of inactivation of healthy cells and effector cells by tumour cells are given by the parameters  $\alpha_{21}$  and  $\alpha_{31}$ , respectively.

The periodic disturbances  $g(t)$  have been applied to the tumour growth in (1). The periodic disturbances are modeled in the form of

$$g(t) = \begin{cases} A \sin(2\pi ft), & \sin(2\pi ft) \geq 0 \\ 0, & \text{otherwise} \end{cases} \quad (2)$$

with amplitude  $A$  and frequency  $f$ . The positive half cycle of periodic signals have been considered since the use of negative half cycles can lead to the negative values of populations which has no biological meaning. Furthermore, the negative cycles of periodic signals have been deliberately modeled by zero intervals which imply the rest period after each intervention.

Since the studies have shown that the impact of environmental factors such as temperature, radiations, oxygen and nutrition are unavoidable on the tumour growth rate, these environmental fluctuations are represented by  $\xi(t)$  which is Gaussian white noise satisfying the statistical properties  $\langle \xi(t) \rangle = 0$  and  $\langle \xi(t)\xi(s) \rangle = \delta(t-s)$  and  $\epsilon$  is the noise intensity.

## III. ANALYSIS AND NUMERICAL RESULTS

The non-dimensionalized cancer model of (1) has been obtained by following the same rescaling in [11] and the corresponding Itô type stochastic differential equation can be written as

$$\begin{aligned} dx_1 &= (x_1(t)(1 - x_1(t)) - \alpha_{12}x_1(t)x_2(t) - \alpha_{13}x_1(t)x_3(t) + \dots \\ &\quad \dots + g(t)) dt + \epsilon dW(t) \\ dx_2 &= (r_2x_2(t)(1 - x_2(t)) - \alpha_{21}x_1(t)x_2(t)) dt \\ dx_3 &= \left( \frac{r_3x_1(t)x_3(t)}{x_1(t) + k_3} - \alpha_{31}x_1(t)x_3(t) - d_3x_3(t) \right) dt \end{aligned} \quad (3)$$

where  $W(t)$  is the Wiener process and the effect of changing environmental conditions is achieved by replacing  $\xi(t)dt$  with the increments of Wiener process  $dW(t)$  which are Gaussian random variables.

The numerical solution of (3) is obtained by using the Euler-Maruyama method. Table I presents the system parameters involved in (3). The parameter values are chosen as in [11] such that with this parameter set the system exhibits chaotic behavior in the absence of periodic disturbances  $g(t) = 0$  and the environmental fluctuations  $\epsilon = 0$ .

TABLE I  
THE PARAMETER VALUES OF MODEL (3).

$\alpha_{12}$	$\alpha_{13}$	$r_2$	$\alpha_{21}$	$r_3$	$k_3$	$\alpha_{31}$	$d_3$
1	2.5	0.6	1.5	4.5	1	0.2	0.5

The phase portrait of the system (3) for the initial conditions  $(x_1(0), x_2(0), x_3(0)) = (0.4, 0.6, 0.1)$  is shown in Fig. 1 when  $g(t) = 0$  and  $\epsilon = 0$ . As seen from Fig. 1 the cancer model has chaotic behavior in the absence of periodic disturbances.

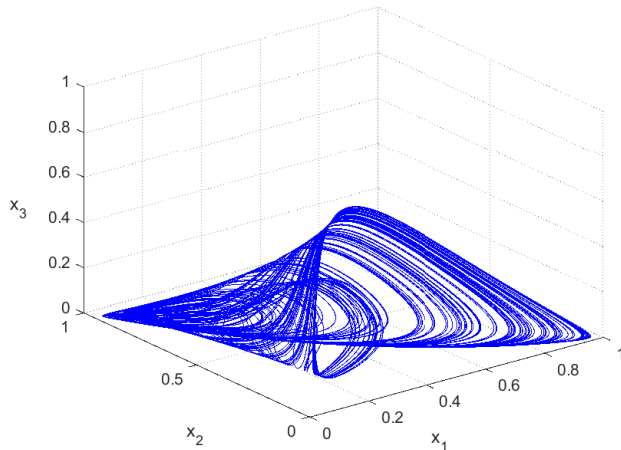


Fig. 1. Chaotic attractor with the initial condition  $x_1(0) = 0.4, x_2(0) = 0.6, x_3(0) = 0.1$  in the absence of periodic disturbances and environmental fluctuations.

However, when the external periodic disturbances are allowed to act during a specific period of time, the evolution of cancer cells can be changed. In this study, in particular, periodic signals are applied at the fundamental frequency and harmonics of the change in the population of tumour cells because under small periodic forces at natural frequencies, a condition known as resonance occurs and the system can produce a large-amplitude response. Further, the effect of oncotripsy is discussed by analyzing how the presence of periodic disturbances at the fundamental frequency and harmonics of the change in the population of tumour cells affects the chaotic nature of the system.

The fundamental frequency of the change in the population of tumour cells is estimated by calculating the amplitude spectrum of system state  $x_1$  of (3) for  $g(t) = 0$  and  $\epsilon = 0$ . The amplitude spectrum has a continuous broadband spectrum due to the chaotic nature and the fundamental frequency also known as the first harmonic is indicated as a maximum in the spectrum. The spectrum is also characterized by several peaks at other relatively high frequencies which refer to the harmonic frequencies. From the amplitude spectrum, the fundamental frequency is estimated as 0.022 Hz and higher harmonics are estimated as 0.0356, 0.0572 Hz, 0.069 Hz, and 0.0756 Hz, respectively.

The responses of the system states are obtained by using the Euler-Maruyama scheme with step size 0.01. The numerical

simulations are performed with 500000-time steps for the initial conditions of the system states  $x_1(0) = 0.4, x_2(0) = 0.6$  and  $x_3(0) = 0.1$  and the noise intensity  $\epsilon = 0.0001$ . The first 10000-time points are ignored to avoid the transient portion of the data.

The frequency of the periodic signal is set to  $f = 0.022$  Hz which is the value of the fundamental frequency of the change in the population of tumour cells. Then to determine the values of amplitude parameter of periodic signal  $A$  at which a qualitative change occurs in the dynamics of cancer cells, the bifurcation diagram of the system (3) is obtained by recording the local maxima  $x_2$  for the range of  $A = [0, 0.2]$  as shown in Fig. 2. It is seen from Fig. 2 that when the frequency of periodic disturbances is chosen as the fundamental frequency, a transition occurs from chaos to periodicity in the dynamics of the chaotic cancer model.

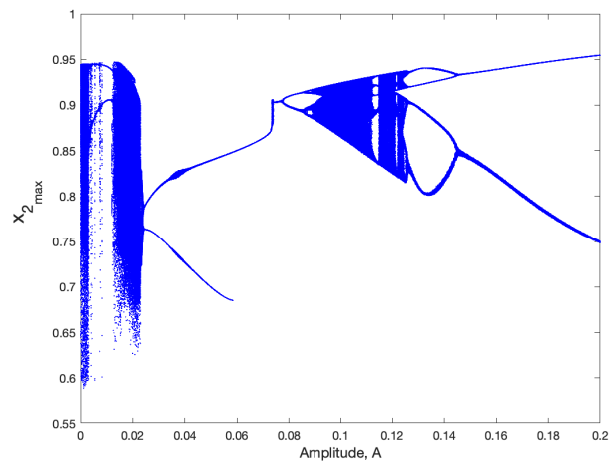


Fig. 2. Bifurcation diagram of model (3) with respect to the bifurcation parameter  $A$ . The frequency of periodic signal is chosen as the fundamental frequency of the change in the population of tumour cells,  $f = 0.022$  Hz.

The bifurcation diagram in Fig. 2 can be explored in more detail by zooming into the various regions of amplitude  $A$ . Figures 3a-3c show the zoomed plots on the particular portions of the bifurcation diagram. It is observed that the system of (3) exhibits rich dynamics such as period-doubling, period-halving and chaotic regions by tuning the amplitude parameter  $A$  in the presence of periodic disturbances with the fundamental frequency of the change in the population of tumour cells.

Consider the bifurcation diagram given in Fig. 3a. When the amplitude parameter  $A$  is in the range  $[0, 0.004)$ , the system has chaotic behavior. If the amplitude parameter  $A$  exceeds some threshold levels such as  $A \approx 0.004$  then the chaos disappears and a period-2 limit cycle occurs. As the amplitude parameter  $A$  increases, the periodic solution becomes unstable and the chaos appears again. Then consider the bifurcation diagram given in Fig. 3b. When the amplitude parameter  $A$  approaches 0.0230, chaos disappears suddenly and period-8 limit cycles occur. As the amplitude parameter  $A$  increases, a very narrow chaotic window appears again with  $A$  in the range  $[0.0233, 0.0240)$  as shown in Fig. 3b.

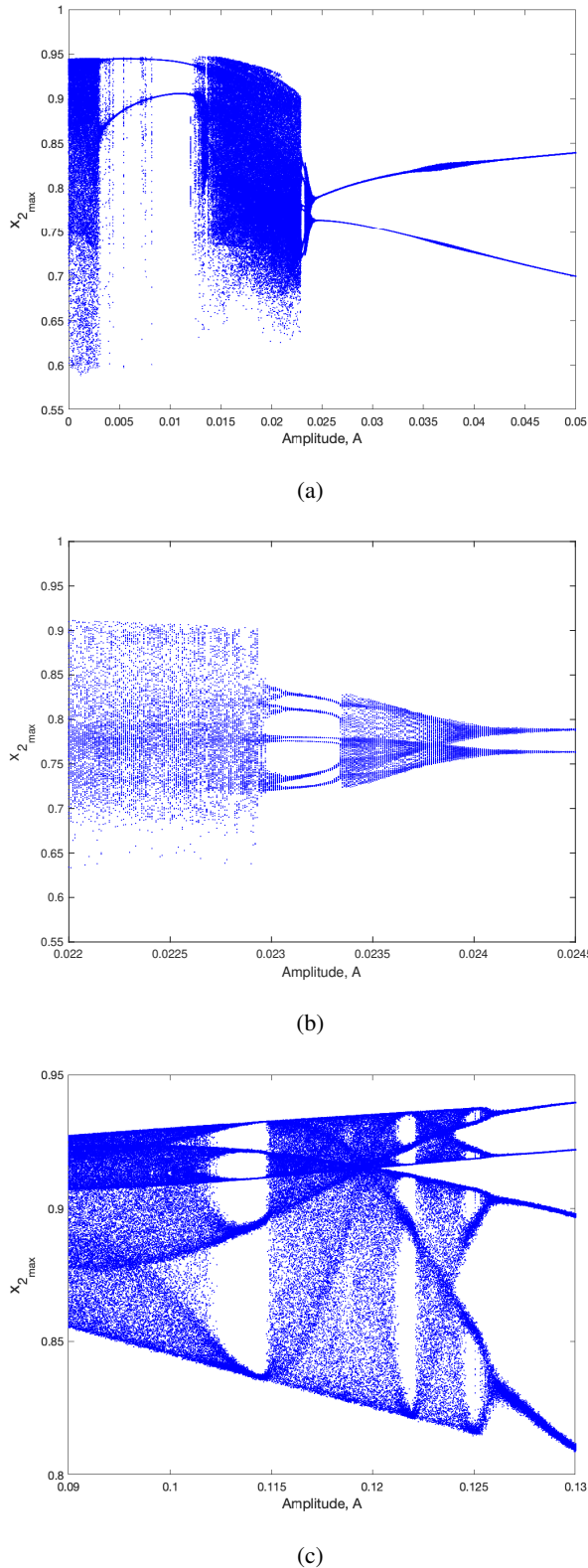


Fig. 3. Bifurcation diagram: Plot of local maxima of  $x_2$  using the amplitude of periodic signal as the bifurcation parameter. The frequency of periodic signal is chosen as the fundamental frequency of the change in the population of tumour cells,  $f = 0.022$  Hz. The amplitude of periodic signal is chosen in the range (a)  $A = [0, 0.05]$  (b)  $A = [0.022, 0.0245]$  (c)  $A = [0.09, 0.13]$ .

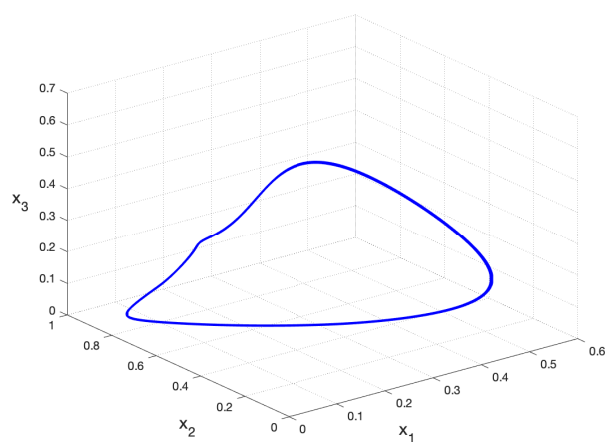
After that, the transition from chaos to the period-2 limit cycle is observed at  $A \approx 0.0240$  and the period-2 limit cycle remains in the region which corresponds to the values of  $A$  in the range  $[0.0240, 0.058)$ . A period-halving bifurcation occurs when  $A$  approaches 0.058 as shown in Fig. 2 which means that a period-2 limit cycle disappears and a period-1 limit cycle appears at this point.

With the increase of the amplitude parameter  $A$  period-doubling bifurcations lead to limit cycles with period 2 and period 4 for  $A \in [0.07728, 0.087)$  and  $A \in [0.087, 0.09)$ , respectively. When  $A$  is increased to the range  $[0.09, 0.126)$ , it can be seen from Fig. 3c that the system (3) has chaotic behavior at a large range of parameter  $A$ , except for three narrow ranges  $[0.112, 0.1115)$ ,  $[0.1217, 0.122)$  and  $[0.124, 0.126)$  which correspond to the limit cycles with periods 5, 6 and 8 respectively. As  $A$  approaches 0.0126 the system (3) evolves into a periodic state through the period-halving bifurcations which result in limit cycles with period 4 and period 2 for  $A \in [0.126, 0.145)$  and  $A \in [0.145, 0.2]$ , respectively as shown in Fig. 2.

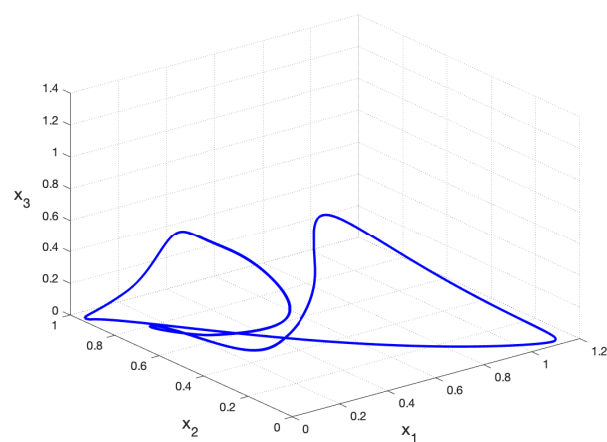
Table II presents the dynamical behaviors of the system (3) with the change of amplitude parameter  $A$  which are obtained through the bifurcation analysis. The phase portraits of the system (3) with different amplitude values of  $A$  are shown in Fig. 4.

TABLE II  
THE DYNAMICS OF SYSTEM (3) FOR THE RANGE OF AMPLITUDE  $A$  WHEN THE FREQUENCY IS SET TO  $f = 0.022$  Hz.

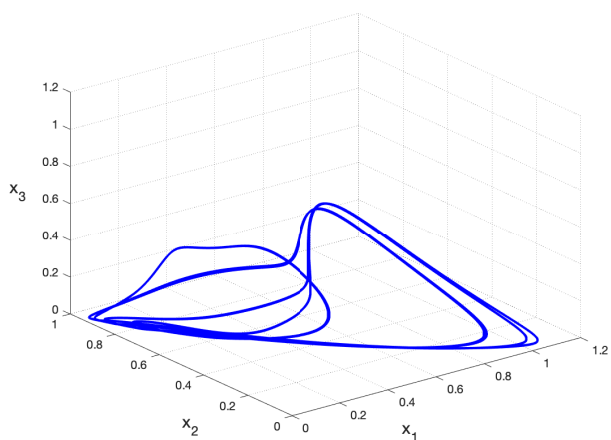
Range of $A$	Attractor of the system
$[0, 0.004)$	Chaotic
$[0.004, 0.0125)$	Period-2 limit cycle
$[0.0125, 0.0230)$	Chaotic
$[0.0230, 0.0233)$	Period-8 limit cycle
$[0.0233, 0.0240)$	Chaotic
$[0.0240, 0.058)$	Period-2 limit cycle
$[0.058, 0.07728)$	Period-1 limit cycle
$[0.07728, 0.087)$	Period-2 limit cycle
$[0.087, 0.09)$	Period-4 limit cycle
$[0.09, 0.112)$	Chaotic
$[0.112, 0.115)$	Period-5 limit cycle
$[0.115, 0.1217)$	Chaotic
$[0.1217, 0.1222)$	Period-6 limit cycle
$[0.1222, 0.124)$	Chaotic
$[0.124, 0.126)$	Period-8 limit cycle
$[0.126, 0.145)$	Period-4 limit cycle
$[0.145, 0.2]$	Period-2 limit cycle



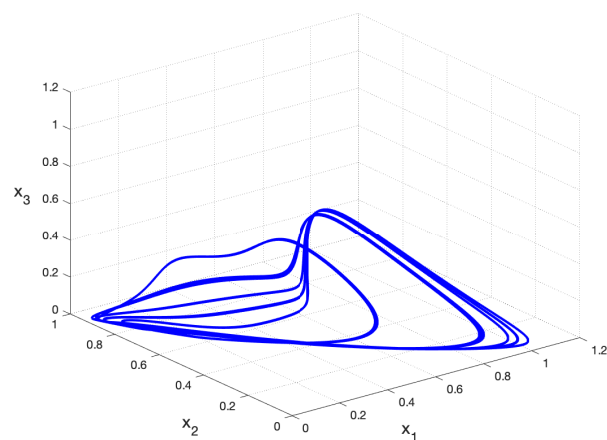
(a)



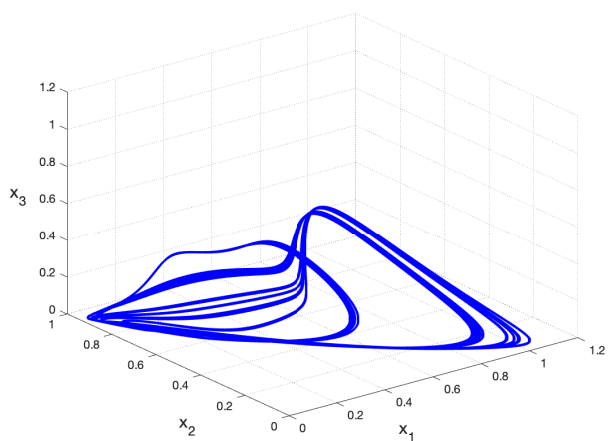
(b)



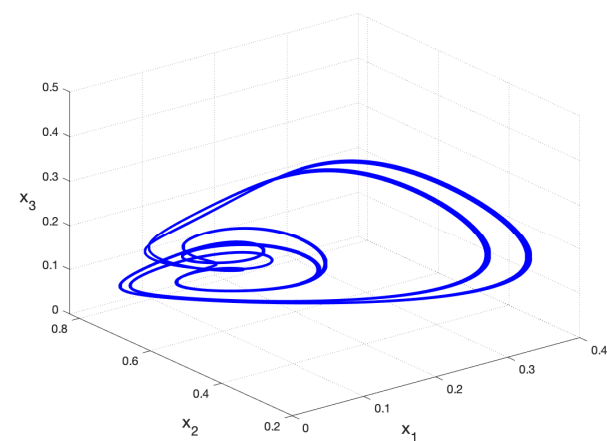
(c)



(d)



(e)



(f)

Fig. 4. 3D phase portrait of system (3) in the presence of periodic disturbances with the frequency  $f = 0.022$  Hz and the amplitude (a)  $A = 0.064$  (b)  $A = 0.2$  (c)  $A = 0.13$  (d)  $A = 0.114$  (e)  $A = 0.122$  (f)  $A = 0.125$ .

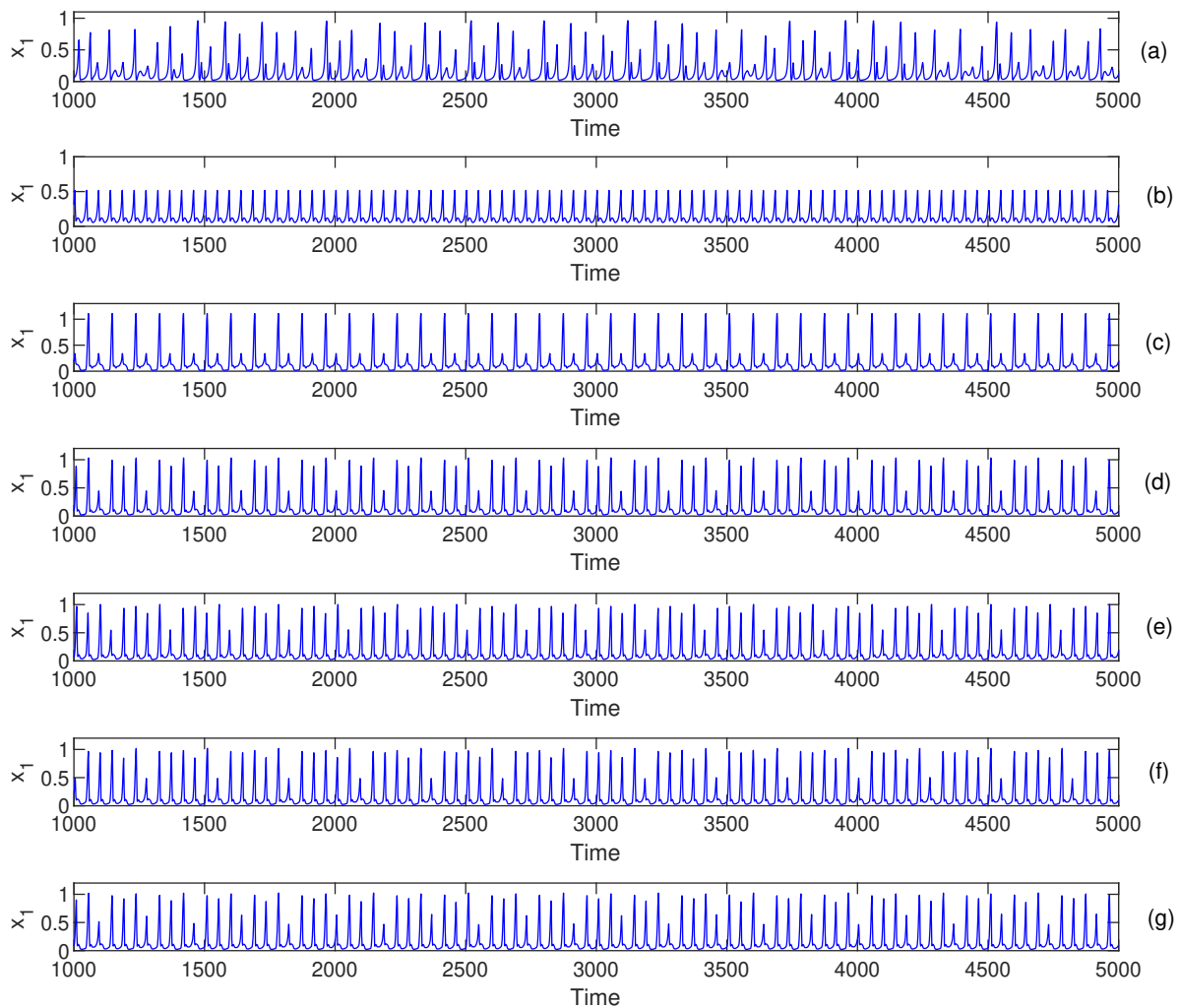


Fig. 5. Time response of the system state  $x_1$  in the absence of periodic disturbances (a)  $A = 0$ ,  $\epsilon = 0$  and when the periodic disturbances are present with the frequency  $f = 0.022$  Hz,  $\epsilon = 0.0001$  and the amplitude (b)  $A = 0.064$  (c)  $A = 0.2$  (d)  $A = 0.13$  (e)  $A = 0.114$  (f)  $A = 0.122$  (g)  $A = 0.125$ .

Time responses of the state  $x_1$  are illustrated in Fig. 5 for the initial conditions  $x_1(0) = 0.4$ ,  $x_2(0) = 0.6$ ,  $x_3(0) = 0.1$ . It is seen from Fig. 5 that the solutions of the system have periodic behaviors when the external periodic disturbances are applied at the fundamental frequency with an appropriate amplitude.

In addition, to analyze the sensitivity to the initial conditions, the parameters of the amplitude and frequency of periodic disturbances are set to  $A = 0.064$  and  $f = 0.022$  Hz which lead to a period-1 limit cycle behavior of the system. Then the bifurcation diagrams of the system (3) are obtained by changing the initial condition of each state separately as shown in Fig. 6. Each of the initial conditions ( $x_1(0)$ ,  $x_2(0)$ ,  $x_3(0)$ ) are varied at the range  $[0.1, 1]$  while the others are set to 0.4. It is seen from Fig. 6 that the period-1 limit cycle behavior of the system remains unchanged with the change of initial conditions  $x_1(0)$ ,  $x_2(0)$  and  $x_3(0)$ .

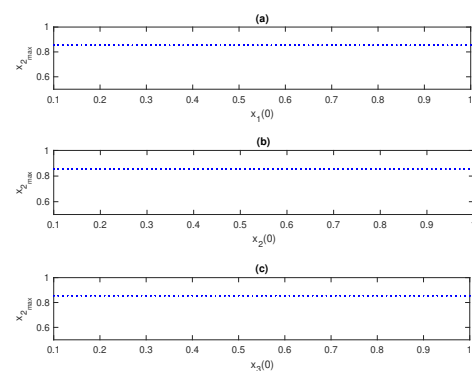


Fig. 6. Bifurcation diagrams with the change of initial conditions: (a)  $x_1(0)$  (b)  $x_2(0)$  (c)  $x_3(0)$ .

The frequency of the periodic signal is set to the second harmonics of the change in the population of tumour cells  $f = 0.0356$  Hz and the corresponding bifurcation diagram shown in Fig. 7a is obtained by recording the local maxima  $x_2$  for the range of  $A = [0, 0.5]$ . Fig. 7b shows the zoomed plot of bifurcation diagram on the range of  $A = [0, 0.05]$ . It can be seen from Fig. 7 that the system of (3) starts from the chaotic state and then suddenly jumps to a periodic state at  $A \approx 0.0076$ . With the amplitude parameter  $A$  in the range  $[0.0076, 0.5]$  the system presents a period-doubling bifurcation followed by a period-halving bifurcation. The dynamic behaviors of the system (3) are given in Table III when the amplitude  $A$  is changed at the specified ranges.

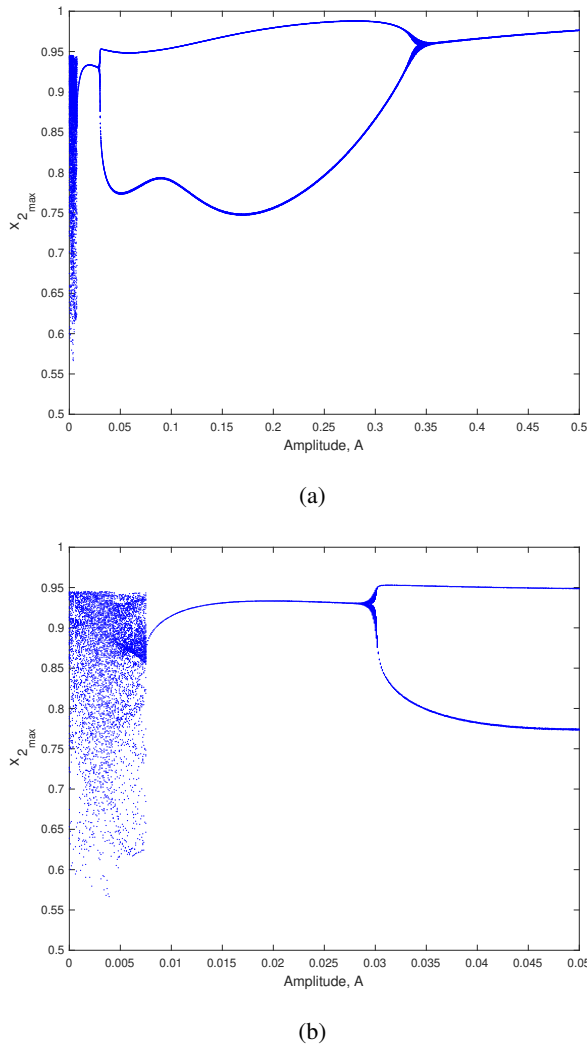


Fig. 7. Bifurcation diagram: Plot of local maxima of  $x_2$  using the amplitude of periodic signal as the bifurcation parameter. The frequency of periodic signal is chosen as the second harmonic of the change in the population of tumour cells  $f = 0.0356$  Hz. The amplitude of periodic signal is chosen in the range (a)  $A = [0, 0.5]$  (b)  $A = [0, 0.05]$ .

Figure 8 presents the phase portraits of system (3) in the presence of periodic disturbances with frequency  $f = 0.0356$  Hz and amplitude  $A = 0.02$  and  $A = 0.04$  for period-1 and period-2 limit cycles, respectively.

TABLE III  
THE DYNAMICS OF SYSTEM (3) FOR THE RANGE OF AMPLITUDE A WHEN THE FREQUENCY IS SET TO  $f = 0.0356$  Hz.

Range of A	Attractor of the system
[0 , 0.0076)	Chaotic
[0.0076 , 0.0297)	Period-1 limit cycle
[0.0297 , 0.3412)	Period-2 limit cycle
[0.3412 , 0.5]	Period-1 limit cycle

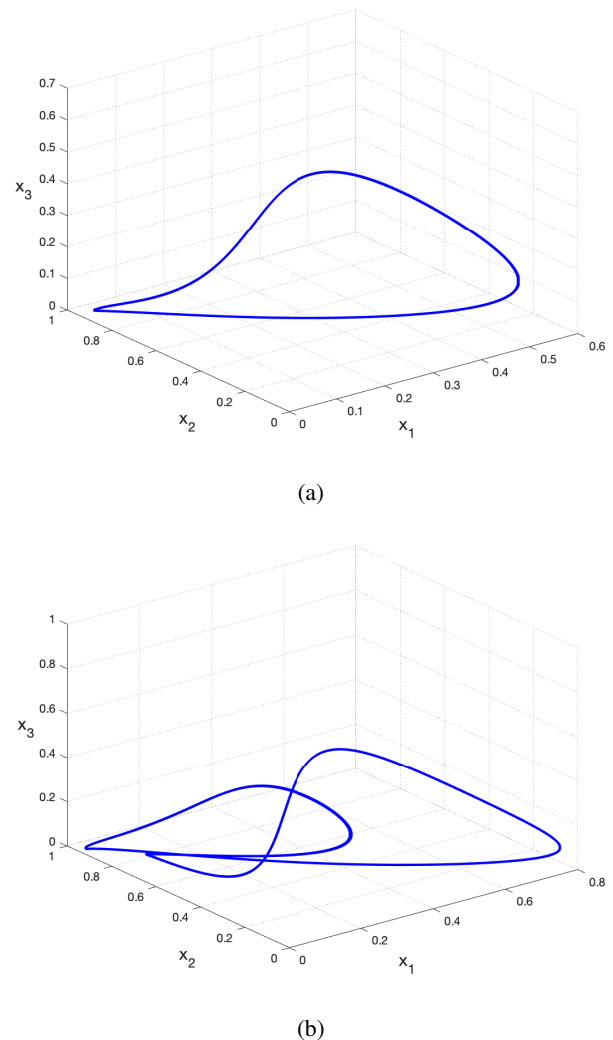
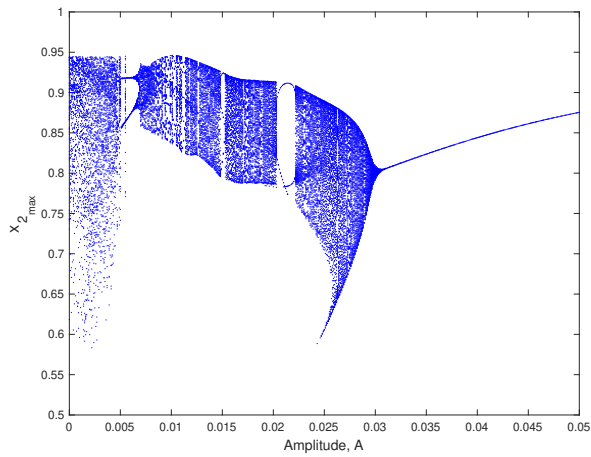
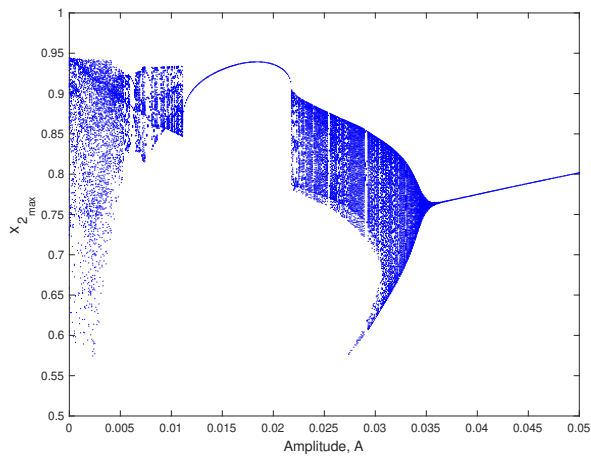


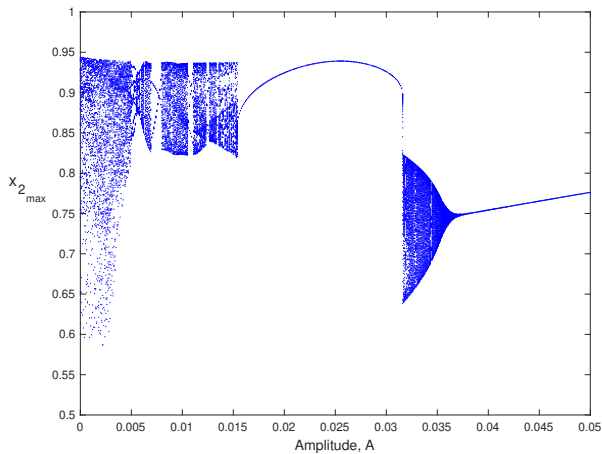
Fig. 8. 3D phase portrait in the presence of periodic disturbances with frequency  $f = 0.0356$  Hz and amplitude (a)  $A = 0.02$  (b)  $A = 0.04$ .



(a)



(b)



(c)

Fig. 9. Bifurcation diagram: Plot of local maxima of  $x_2$  using the amplitude of periodic signal as the bifurcation parameter. The frequency of periodic signal is chosen as the (a) 3rd harmonic  $f = 0.0572$  Hz (b) 4th harmonic  $f = 0.069$  Hz and (c) 5th harmonic  $f = 0.0756$  Hz.

TABLE IV  
THE DYNAMICS OF SYSTEM FOR THE RANGE OF AMPLITUDE  $A$  WHEN THE FREQUENCY IS SET TO  $f = 0.0572$  Hz.

Range of $A$	Attractor of the system
$[0, 0.0052)$	Chaotic
$[0.0052, 0.0066)$	Period-2 limit cycle
$[0.0066, 0.0149)$	Chaotic
$[0.0149, 0.0152)$	Period-2 limit cycle
$[0.0152, 0.0204)$	Chaotic
$[0.0204, 0.022)$	Period-2 limit cycle
$[0.022, 0.0309)$	Chaotic
$[0.0309, 0.05]$	Period-1 limit cycle

TABLE V  
THE DYNAMICS OF SYSTEM FOR THE RANGE OF AMPLITUDE  $A$  WHEN THE FREQUENCY IS SET TO  $f = 0.069$  Hz.

Range of $A$	Attractor of the system
$[0, 0.006)$	Chaotic
$[0.006, 0.0063)$	Period-3 limit cycle
$[0.0063, 0.0075)$	Chaotic
$[0.0075, 0.0079)$	Period-4 limit cycle
$[0.0079, 0.0112)$	Chaotic
$[0.0112, 0.0218)$	Period-1 limit cycle
$[0.0218, 0.0375)$	Chaotic
$[0.0375, 0.05]$	Period-1 limit cycle

TABLE VI  
THE DYNAMICS OF SYSTEM FOR THE RANGE OF AMPLITUDE  $A$  WHEN THE FREQUENCY IS SET TO  $f = 0.0756$  Hz.

Range of $A$	Attractor of the system
$[0, 0.007)$	Chaotic
$[0.007, 0.0079)$	Period-2 limit cycle
$[0.0079, 0.0155)$	Chaotic
$[0.0155, 0.0315)$	Period-1 limit cycle
$[0.0315, 0.0387)$	Chaotic
$[0.0387, 0.05]$	Period-1 limit cycle

When the periodic disturbances are applied at the higher harmonics up to the 5th harmonic, the corresponding bifurcation diagrams for the amplitude parameter  $A$  in the range  $[0, 0.05]$  as shown in Fig. 9. It can be seen from Fig. 9 that the system (3) evolves from chaotic into a periodic state by tuning the amplitude of periodic disturbances. It can be also seen that chaotic regions contain some very narrow periodic windows and when the frequency is set to the higher harmonics there are successive transitions from chaotic to periodic state or periodic to chaotic state as the amplitude

of the periodic disturbances gradually increases. Through bifurcation analysis, the amplitude of periodic disturbances to observe the periodic dynamics such as period-1 limit cycle can be also clearly specified.

Table IV, Table V and Table VI present the ranges of the amplitude  $A$  which correspond to the regions of periodic and chaotic behaviors when the frequency of periodic disturbances is set to  $f = 0.0572$  Hz,  $f = 0.069$  Hz and  $f = 0.0756$  Hz, respectively.

Figure 10 shows the phase portraits of the system (3) when the amplitude of periodic disturbances is set to  $A = 0.04$  and the frequency of periodic disturbances is tuned to the values of 3rd, 4th and 5th harmonics. Figure 11 shows the structures of period-2 limit cycles when the periodic disturbances are applied at 3rd and 5th harmonics with a sufficient amplitude such as  $A = 0.021$  and  $A = 0.0075$ , respectively.

It is seen from Fig. 10 that the system exhibits period-1 limit cycles for those frequencies and a change in the frequency results in a change in the amplitude of the limit cycles. It is also observed that not only the amplitude of the limit cycle but also the period of the limit cycle can be changed with the change of frequency of periodic disturbances.

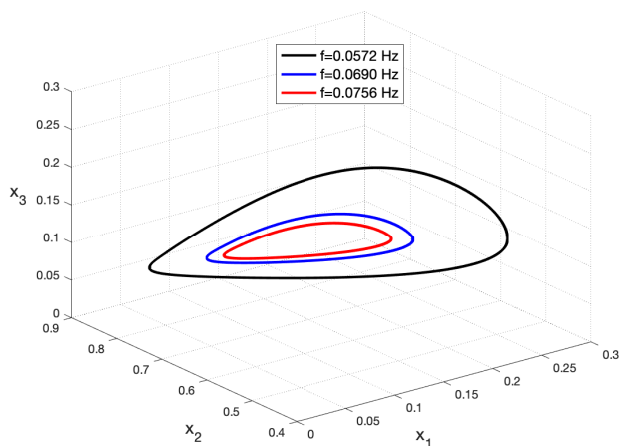


Fig. 10. 3D phase solution in the presence of periodic disturbances with amplitude  $A = 0.04$  and the frequency  $f = 0.0572$  Hz (black line);  $f = 0.069$  Hz (blue line);  $f = 0.0756$  Hz (red line).

Specifically, by choosing the frequency of periodic disturbances as 1st or 2nd harmonic the system exhibits period-2 limit cycles at  $A = 0.04$ . Thus, the system exhibits different sensitivities to the same amplitude of periodic disturbances depending on the frequency of periodic disturbances.

Therefore, it can be concluded that the chaotic cancer model (3) is highly dependent on the frequency of periodic disturbances. This just ensures that if the tumour cells are disturbed with a periodic signal at the fundamental frequency or harmonics, the dynamics of the system can be switched from chaotic to periodic behavior.

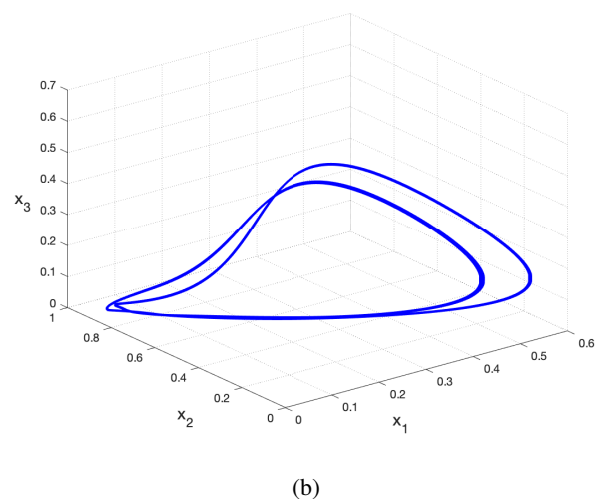
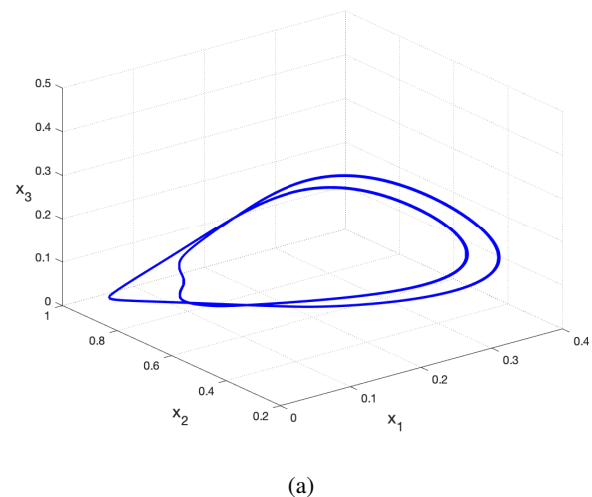


Fig. 11. 3D phase solution in the presence of periodic disturbances when the frequency  $f$  and amplitude  $A$  are set to (a)  $f = 0.0572$  Hz and  $A = 0.021$  (b)  $f = 0.0756$  Hz and  $A = 0.0075$ .

#### IV. CONCLUSION

In this study, the method of oncotripsy is discussed to stabilize chaotic behavior in a cancer model. To analyze the effect of the resonance phenomenon on the chaotic cancer model, the fundamental and higher harmonic frequencies of the change in the tumour cell population have been calculated, and the external periodic disturbances have been applied at those frequencies to the tumour growth. The amplitude of periodic disturbances has been considered as the bifurcation parameter, and the associated bifurcation diagrams have been obtained for each of the harmonics. The numerical results have been utilized to obtain the dynamic responses of the system.

It has been observed that when the periodic disturbances are applied at the fundamental frequency, the chaotic system can be stabilized to a limit cycle with period-one. Moreover, when the frequency is set to the fundamental frequency of the change in the population of tumour cells, the system may have rich dynamic behaviors such as limit cycles exhibiting different periods just by tuning the amplitude parameter. An

interesting phenomenon has been observed when the frequency of the periodic disturbances is chosen as the second harmonics of the change in the population of tumour cells. In this case, the system has a very narrow chaotic region, and as the amplitude of periodic disturbances exceeds some low level, then the chaos disappears, and the periodic behaviors occur. Furthermore, when the frequency is set to higher harmonics, it has been observed that the dynamics of the system can be switched between chaotic and periodic states with the change of the amplitude parameter.

Finally, it is important to note that our results also provide insights on a possible effect of oncotripsy for the stabilization of chaos in a cancer model. Periodic disturbances acting on a chaotic cancer model are capable of exhibiting periodic behaviors, which may help adjust treatment regimes. Therefore, it will be extremely important to understand the parameters and conditions that lead to limit cycles.

#### DATA AVAILABILITY

All figures were generated using MATLAB R2021b.

#### REFERENCES

- [1] S. G. Orel and M. D. Schnall, "Mr imaging of the breast for the detection, diagnosis, and staging of breast cancer," *Radiology*, vol. 220, no. 1, pp. 13–30, 2001.
- [2] C. K. Kuhl, S. Schrading, C. C. Leutner, N. Morakkabati-Spitz, E. Wardelmann, R. Fimmers, W. Kuhn, and H. H. Schild, "Mammography, breast ultrasound, and magnetic resonance imaging for surveillance of women at high familial risk for breast cancer," *Journal of clinical oncology*, vol. 23, no. 33, pp. 8469–8476, 2005.
- [3] S. Vedantham, A. Karellas, G. R. Vijayaraghavan, and D. B. Kopans, "Digital breast tomosynthesis: state of the art," *Radiology*, vol. 277, no. 3, pp. 663–684, 2015.
- [4] A. R. Celik, M. B. Kurt, and S. Helhel, "An experimental performance investigation of an ultra-wideband directional antenna in the microwave imaging of breast cancer tumor," *The Applied Computational Electromagnetics Society Journal (ACES)*, pp. 1549–1560, 2019.
- [5] V. A. Kuznetsov, I. A. Makalkin, M. A. Taylor, and A. S. Perelson, "Nonlinear dynamics of immunogenic tumors: parameter estimation and global bifurcation analysis," *Bulletin of mathematical biology*, vol. 56, no. 2, pp. 295–321, 1994.
- [6] D. Kirschner and J. C. Panetta, "Modeling immunotherapy of the tumor-immune interaction," *Journal of mathematical biology*, vol. 37, no. 3, pp. 235–252, 1998.
- [7] V. A. Kuznetsov and G. D. Knott, "Modeling tumor regrowth and immunotherapy," *Mathematical and Computer Modelling*, vol. 33, no. 12-13, pp. 1275–1287, 2001.
- [8] L. G. De Pillis and A. Radunskaya, "The dynamics of an optimally controlled tumor model: A case study," *Mathematical and computer modelling*, vol. 37, no. 11, pp. 1221–1244, 2003.
- [9] A. d'Onofrio, "A general framework for modeling tumor-immune system competition and immunotherapy: Mathematical analysis and biomedical inferences," *Physica D: Nonlinear Phenomena*, vol. 208, no. 3-4, pp. 220–235, 2005.
- [10] L. G. de Pillis, W. Gu, and A. E. Radunskaya, "Mixed immunotherapy and chemotherapy of tumors: modeling, applications and biological interpretations," *Journal of theoretical biology*, vol. 238, no. 4, pp. 841–862, 2006.
- [11] M. Itik and S. P. Banks, "Chaos in a three-dimensional cancer model," *International Journal of Bifurcation and Chaos*, vol. 20, no. 01, pp. 71–79, 2010.
- [12] H.-C. Wei and J.-T. Lin, "Periodically pulsed immunotherapy in a mathematical model of tumor-immune interaction," *International Journal of Bifurcation and Chaos*, vol. 23, no. 04, p. 1350068, 2013.
- [13] J. Yang, S. Tang, and R. A. Cheke, "Modelling pulsed immunotherapy of tumour-immune interaction," *Mathematics and Computers in Simulation*, vol. 109, pp. 92–112, 2015.
- [14] Y. Xu, J. Feng, J. Li, and H. Zhang, "Stochastic bifurcation for a tumor-immune system with symmetric lévy noise," *Physica A: Statistical Mechanics and its Applications*, vol. 392, no. 20, pp. 4739–4748, 2013.
- [15] M. Baar, L. Coquille, H. Mayer, M. Hölzel, M. Rogava, T. Tüting, and A. Bovier, "A stochastic model for immunotherapy of cancer," *Scientific reports*, vol. 6, no. 1, pp. 1–10, 2016.
- [16] X. Liu, Q. Li, and J. Pan, "A deterministic and stochastic model for the system dynamics of tumor-immune responses to chemotherapy," *Physica A: Statistical Mechanics and its Applications*, vol. 500, pp. 162–176, 2018.
- [17] X. Li, G. Song, Y. Xia, and C. Yuan, "Dynamical behaviors of the tumor-immune system in a stochastic environment," *SIAM Journal on Applied Mathematics*, vol. 79, no. 6, pp. 2193–2217, 2019.
- [18] J. Yang, Y. Tan, and R. A. Cheke, "Modelling effects of a chemotherapeutic dose response on a stochastic tumour-immune model," *Chaos, Solitons & Fractals*, vol. 123, pp. 1–13, 2019.
- [19] P. Schulthess, V. Rottschäfer, J. W. Yates, and P. H. van Der Graaf, "Optimization of cancer treatment in the frequency domain," *The AAPS journal*, vol. 21, no. 6, p. 106, 2019.
- [20] S. Heyden and M. Ortiz, "Oncotripsy: Targeting cancer cells selectively via resonant harmonic excitation," *Journal of the Mechanics and Physics of Solids*, vol. 92, pp. 164–175, 2016.
- [21] S. K. Jaganathan, A. P. Subramanian, M. V. Vellayappan, A. Balaji, A. A. John, A. K. Jaganathan, and E. Supriyanto, "Natural frequency of cancer cells as a starting point in cancer treatment," *Current Science*, pp. 1828–1832, 2016.
- [22] M. Fraldi, A. Cugno, L. Deseri, K. Dayal, and N. Pugno, "A frequency-based hypothesis for mechanically targeting and selectively attacking cancer cells," *Journal of the Royal Society Interface*, vol. 12, no. 111, p. 20150656, 2015.
- [23] S. Heyden and M. Ortiz, "Investigation of the influence of viscoelasticity on oncotripsy," *Computer Methods in*

*Applied Mechanics and Engineering*, vol. 314, pp. 314–322, 2017.

- [24] E. Calabrò and S. Magazù, “New perspectives in the treatment of tumor cells by electromagnetic radiation at resonance frequencies in cellular membrane channels,” *The Open Biotechnology Journal*, vol. 13, no. 1, 2019.
- [25] U. Lucia, G. Grisolia, A. Ponzetto, L. Bergandi, and F. Silvagno, “Thermomagnetic resonance affects cancer growth and motility,” *Royal Society open science*, vol. 7, no. 7, p. 200299, 2020.
- [26] D. R. Mittelstein, J. Ye, E. F. Schibber, A. Roychoudhury, L. T. Martinez, M. H. Fekrazad, M. Ortiz, P. P. Lee, M. G. Shapiro, and M. Gharib, “Selective ablation of cancer cells with low intensity pulsed ultrasound,” *Applied Physics Letters*, vol. 116, no. 1, p. 013701, 2020.
- [27] D. R. Mittelstein, “Modifying ultrasound waveform parameters to control, influence, or disrupt cells,” Ph.D. dissertation, California Institute of Technology, 2020.
- [28] E. Schibber, D. Mittelstein, M. Gharib, M. Shapiro, P. Lee, and M. Ortiz, “A dynamical model of oncotripsy by mechanical cell fatigue: selective cancer cell ablation by low-intensity pulsed ultrasound,” *Proceedings of the Royal Society A*, vol. 476, no. 2236, p. 20190692, 2020.
- [29] E. Figueroa-Schibber, “High-cycle dynamic cell fatigue with applications on oncotripsy,” Ph.D. dissertation, California Institute of Technology, 2020.
- [30] S. Abernethy and R. J. Gooding, “The importance of chaotic attractors in modelling tumour growth,” *Physica A: Statistical Mechanics and its Applications*, vol. 507, pp. 268–277, 2018.
- [31] M. Fahimi, K. Nouri, and L. Torkzadeh, “Chaos in a stochastic cancer model,” *Physica A: Statistical Mechanics and its Applications*, vol. 545, p. 123810, 2020.

## BIOGRAPHY



**Serpil Yılmaz** is currently an assistant professor of Computer Engineering at İzmir Katip Çelebi University. She received her M.Sc. and Ph.D. degrees in Electronics and Communication Engineering from İzmir Institute of Technology in 2012 and 2019, respectively. Her research interests include chaotic

systems, stochastic models, artificial intelligence and embedded systems.